A Journal of the Gesellschaft Deutscher Chemiker
Angewandte
GDCh
International Edition
Chemie
www.angewandte.org

Accepted Article

Title: Theoretical, Solid-State and Solution Quantification of the Hydrogen Bond Enhanced Halogen Bond

Authors: Daniel A. Decato, Asia Marie S. Riel, James H. May, Vyacheslav S. Bryantsev, and Orion Boyd Berryman

To be cited as: *Angew. Chem. Int. Ed.* 10.1002/anie.202012262

Link to VoR: https://doi.org/10.1002/anie.202012262

WILEY-VCH

10.1002/anie.202012262

WILEY-VCH

RESEARCH ARTICLE

Theoretical, Solid-State and Solution Quantification of the Hydrogen Bond Enhanced Halogen Bond

Daniel A. Decato[a], Asia Marie S. Riel[a], James H. May[a], Vyacheslav S. Bryantsev[b], Orion B. Berryman*[a]

[a] Dr. D.A. Decato, Dr. A.M.S. Riel, J.H. May, Prof. Dr. O.B. Berryman
Department of Chemistry and Biochemistry
University of Montana
132 Campus Drive, Missoula, Montana 59812
E-mail: orion.berryman@umontana.edu
[b] Dr. V.S. Bryantsev
Chemical Sciences Division
Oak Ridge National Laboratory
Oak Ridge, Tennessee 37831, USA.

Supporting information for this article is given via a link at the end of the document.

Abstract: Proximal noncovalent forces are commonplace in natural systems and understanding the consequences of their juxtaposition is critical. This paper experimentally quantifies for the first time a Hydrogen Bond enhanced Halogen Bond (HBeXB) without the complexities of protein structure or preorganization. An HBeXB is a halogen bond that has been strengthened when the halogen donor simultaneously accepts a hydrogen bond. Our theoretical studies suggest that electron-rich halogen bond donors are strengthened most by an adjacent hydrogen bond. Furthermore, stronger hydrogen bond donors enhance the halogen bond the most. X-ray crystal structures of halide complexes (X^- = Br^-, I^-) reveal that HBeXBs produce shorter halogen bonds than non-hydrogen bond analogues. ^{19}F NMR titrations with chloride highlight that the HBeXB analogue exhibits stronger binding. Together, these results form the foundation for future studies concerning hydrogen bonds and halogen bonds in close proximity.

Introduction

Electronegative substituents in polar covalent bonds are usually adept hydrogen bond acceptors. However, terminal organohalogens are paradoxical, as they are considered weak hydrogen bond acceptors.[1] Despite decades of hydrogen bond research, the rationale for this observation remains largely enigmatic.[2] Efforts to understand organohalogens as hydrogen bond acceptors (Figure 1A) have largely focused on fluorine.[3–8] In contrast, the consideration of heavier halogens (that halogen bond: X = Cl, Br, I) has lagged. The few studies of heavy organohalogens as hydrogen bond acceptors have largely been theoretical,[9–11] with only a handful of experimental[12–18] and database[19,20] studies reported. The importance of addressing this deficiency is underscored by the recent proliferation of halogen bonding materials, the ubiquity of the hydrogen bond, and a recent appreciation that hydrogen bonding can significantly influence halogen bonding (*vide infra*). Herein, we examine the intersecting fields of hydrogen and halogen bonding by experimentally quantifying, for the first time, the influence of a hydrogen bond to the electronegative region of a halogen bond donor.

The halogen bond is an attractive noncovalent interaction between an electrophilic halogen and a Lewis base (Figure 1B).[21] The linear interaction has found applications in fundamental and functional chemical disciplines.[22–31] The directionality is often attributed to an anisotropic distribution of electron density that develops on an electron-deficient halogen—an electropositive region at the tip of the halogen projected away from the covalent bond (frequently referred to as the 'σ-hole') and an electronegative belt orthogonal to the covalent bond. The electropositive region is often invoked to explain the attractive interaction with Lewis bases, while the electronegative region has helped explain the linearity of the halogen bond, as well as various "side-on" interactions with electrophilic species.[32,33]

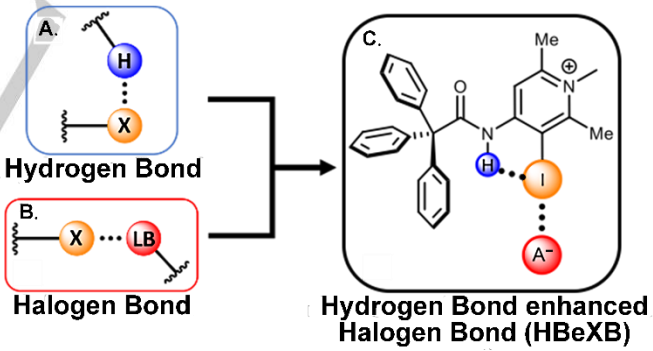

Figure 1. Cartoon depiction of: **A**. hydrogen bond to a halogen atom; **B**. A halogen bond to a Lewis base; **C**. ChemDraw of the model compound for the hydrogen bond enhanced halogen bond studies in this work. X = halogen, LB = Lewis base, H = hydrogen, I = iodine, A^- = anion.

The amphoteric nature of halogen bond donors (X= Cl, Br, I) has led researchers to consider their significance as hydrogen bond acceptors (H•••X—C; Figure 1A) or as halogen bond donors (C—X•••LB; Figure 1B) within ligand-protein complexes. Select examples highlight the remarkable influence of halogens when operating in either role. In one case, a hydrogen bond from an arginine side chain of a hepatitis C virus to a bromine atom (H•••Br—C) of an inhibitor contributed to a 250-fold improvement in efficacy (IC_{50}).[34] A separate study showed that a halogen bond (C—Br•••O) from an inhibitor to a hydroxyl oxygen of a threonine

contributed to a > 1000- fold selectivity (IC_{50}) of aldose reductase over the closely related aldehyde reductase.[35] These contrasting examples echo conflicting findings of recent Protein Data Bank and theoretical studies. Here, one group has suggested that the halogen bond (C—X•••O) is more important to ligand-protein binding,[36,37] while another has suggested that the hydrogen bond to the halogen (H•••X—C) is more significant.[38] Differences aside, the implications are that both interactions (halogen bonds and hydrogen bonds to halogens) are understudied, yet can remarkably influence binding, selectivity, and molecular structure.

While both groups above noted the potential for organohalogens to simultaneously operate as a hydrogen bond acceptor and halogen bond donor, they did not consider how these interactions influence each other nor the potential consequences on molecular structure. In this light, we have recently investigated the Hydrogen Bond enhanced Halogen Bond (HBeXB; Figure 1C).[39] Under these conditions, a hydrogen bond to the electronegative belt of a halogen bond donor further polarizes and strengthens the halogen bond donor. An HBeXB can significantly influence both macromolecule stability and small molecule binding. In one case, the Ho group engineered a *meta*-chlorotyrosine (HBeXB donor) into T4 lysozyme which increased the thermal stability and activity of the enzyme at elevated temperatures compared to the parent enzyme.[40] Concurrently, our lab demonstrated that a hydrogen bond to a halogen bond donor can preorganize molecular structure and augment halogen bond strength in bidentate anion receptors—leading to a near 9-fold increase in halide binding.[41] These seminal studies provided proof-of-concept, yet the complexities of protein structure and anion receptor preorganization effects obscured quantification of just the HBeXB. Thus, we designed a model system with isolated HBeXBs that allowed us to quantify the HBeXB in solution, the solid-state and *in silico*.

Results and Discussion

Design considerations

Model compounds designed to study the HBeXB included a halogen bond donor adjacent to a sterically shielded hydrogen bond donor (Figure 1C). The iodine halogen bond donor was attached to an electron-deficient pyridinium ring to strengthen the halogen bond donor and ensured the presence of an anion in solid-state evaluations. The amide hydrogen bond donor was incorporated proximal to the iodine to form a 5-membered intramolecular hydrogen bond ring (Figure 1C). A trityl group flanking the amide proton provided sufficient steric hindrance to prevent intermolecular hydrogen bonding. The effectiveness of this functional group arrangement has been described in several reports by Li and coworkers, who noted that five-membered N–H•••X (X = Cl, Br, I) hydrogen bonding rings were more stable than six-membered rings in aromatic amides.[42–44] A charge-assisted C–H hydrogen bond donor *ortho* to the amide substituent was designed to reduce conformational flexibility by intramolecular hydrogen bonding to the amide carbonyl oxygen. Furthermore, functionalizing the positions *ortho* to the pyridinium nitrogen enabled evaluation of substituent effects on the HBeXB and limited intermolecular C–H hydrogen bonding. Neutral compounds with trifluorophenyl as the electron-withdrawing group were also assessed. Lastly, ester derivatives lacking a hydrogen bond donor were employed for comparison. Combined, these compounds represent four systematically altered pairs of HBeXB (amides) and non-hydrogen bonding (esters) molecules—three pairs of pyridinium compounds (**1** & **2**, **3** & **4**, **5** & **6**; Figure 2) and one neutral pair (**7** & **8**; Figure 3).

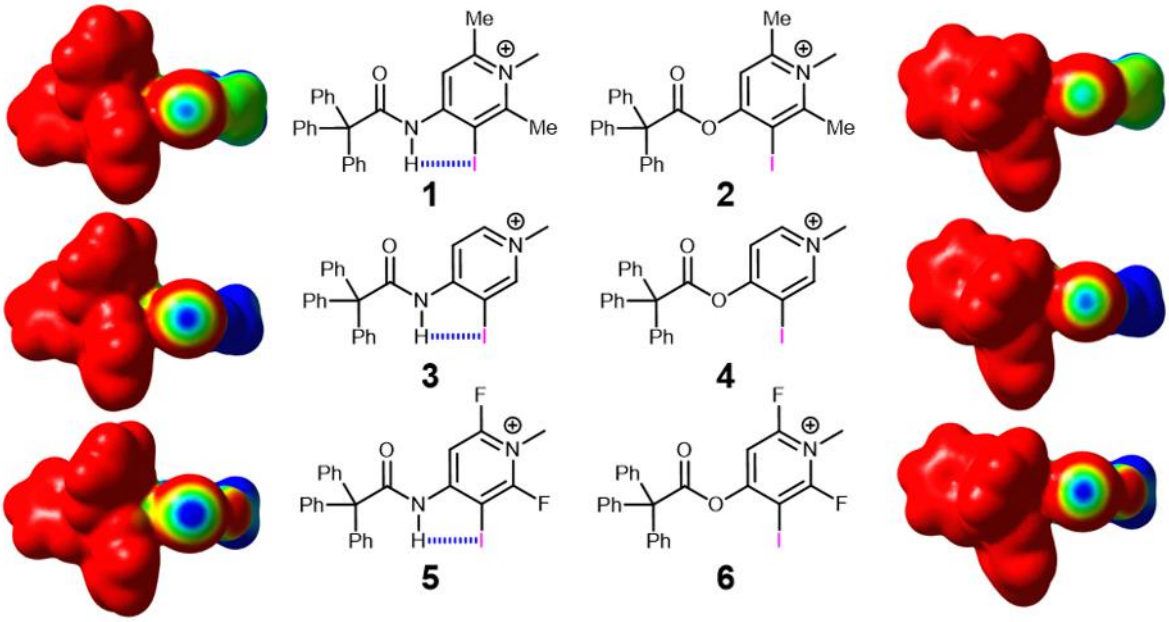

Figure 2. Molecular electrostatic potential surfaces (isovalue = 0.001 a.u.) for pyridinium based HBeXB (**1, 3, 5**) and non-hydrogen bond (**2, 4, 6**) derivatives. The differences in $V_{s,max}$ values located on iodine donors of isostructural pyridinium rings are as follows **1** & **2** = 3.77; **3** & **4** = 3.76; **5** & **6** = 3.13 (all values in kcal/mol). All ESP maps are displayed on the same scale. Electron-deficient regions are blue and electron-rich regions are red.

10.1002/anie.202012262

Computational evaluations

Pyridinium halogen bonding compounds **1–6** (Figure 2) were evaluated using gas-phase density functional theory. Using Gaussian 09,[45] calculations were performed using the B3LYP, M06-2X, and ωB97-XD functionals with the def2-TZVPP basis set for all atoms and the small-core energy-consistent relativistic effective core potential (def2-ECP) applied to iodine. A smaller basis set was also evaluated for comparison using the B3LYP functional with the 6-31+G (d,p) basis set for all atoms except iodine. In this case, the LANL2DZdp and large-core effective core potential were used to model iodine (for additional computational details see SI). The amide and ester conformations are most similar in the B3LYP/def2-TZVPP calculations and thus initial discussions focus on these calculations. The results from the other functionals and the smaller basis set with B3LYP are discussed at the end of the computational sections.

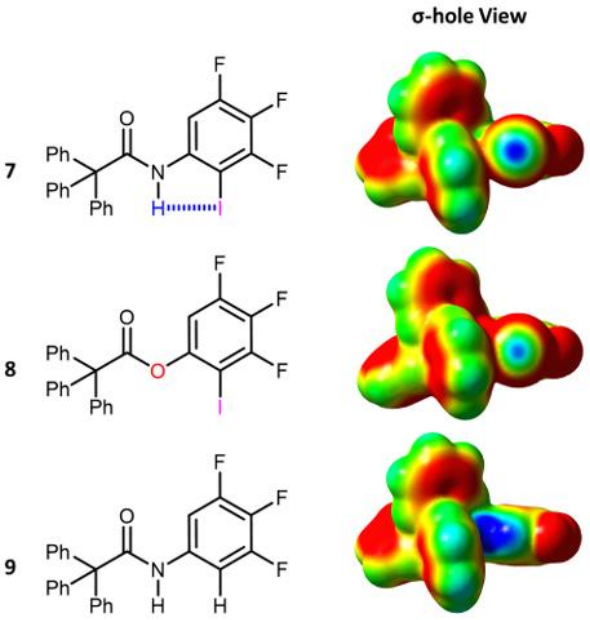

Figure 3. Molecular electrostatic potential surfaces (isovalue = 0.001 a.u.) for trifluorophenyl HBeXB (**7**), non-hydrogen bonding derivative (**8**), and non-halogen bonding control (**9**) The ESP maps are displayed on the same scale. Electron-deficient regions are blue and electron-rich regions are red.

Molecular electrostatic potential analysis

Molecular electrostatic potential maps of **1–6** were calculated to provide an estimate of halogen bond strength by assessing the σ-hole ($V_{s,max}$) of the iodine donors (Figure 2). As expected, derivatives with electron withdrawing fluorine substituents (**5** & **6**) had the most positive $V_{s,max}$, followed by the hydrogen (**3** & **4**) and methyl (**1** & **2**) derivatives (Figure 2), respectively. The $V_{s,max}$ values span 11.55 kcal/mol (difference between **5** and **2**, B3LYP/def2-TZVPP) reiterating that substituents can be used to modulate the halogen bond ($V_{s,max}$) in charge assisted pyridinium donors.

To probe how an adjacent hydrogen bond influences the halogen bond, amide derivatives (**1**, **3** & **5**) were compared to isostructural ester derivatives (**2**, **4** & **6**). Specifically, the $V_{s,max}$ of the σ-holes for HBeXB derivatives (**1**, **3,** & **5**)—with an adjacent hydrogen bond—are more positive by 3.58–3.89 kcal/mol compared to the isostructural non-hydrogen bonding ester controls (**2**, **4**, & **6**; Table 1, B3LYP/def2-TZVPP). The largest difference between the amide/ester pairs occurred between the most electron-rich analogues (**1** & **2**). Considering this, a relatively electron-rich pair of charge-neutral trifluorophenyl halogen bonding derivatives (**7** & **8**) were also evaluated. Here, an even greater difference in $V_{s,max}$ was observed (4.52 kcal/mol) between the HBeXB and the non-hydrogen bond derivative (**7** and **8**, Figure 3). *Thus, the adjacent hydrogen bond has a larger influence on the more electron-rich halogen bond donors.*

Table 1. Calculated energy differences between isostructural HBeXB and non-hydrogen bonding derivatives

		Molecule							
Parameter	**Computational method**	**1**	**2**	**3**	**4**	**5**	**6**	**7**	**8**
$\Delta V_{s,max}$	B3LYP/def2-TZVPP	3.89		3.58		3.58		4.52	
	M06-2X/def2-TZVPP	1.76		2.07		4.14		5.52	
	ωB97-XD/def2-TZVPP	2.57		3.58		4.58		5.08	
	B3LYP/6-31+G(d,p)/LANL2DZdp	3.77		3.76		3.13		4.45	
Δ IE*	B3LYP/def2-TZVPP	-1.01		-0.47		-0.17		-1.44	
	M06-2X/def2-TZVPP	-1.81		-0.95		-0.56		-0.84	
	ωB97-XD/def2-TZVPP	-1.76		-1.30		-0.72		-1.54	
	B3LYP/6-31+G(d,p)/LANL2DZdp	-1.57		-1.09		-0.86		-1.59	
Δ CE**	B3LYP/def2-TZVPP	-2.37		-2.10		-2.46		-1.65	
	M06-2X/def2-TZVPP	-2.65		-2.51		-3.08		-1.66	
	ωB97-XD/def2-TZVPP	-2.88		-2.79		-3.39		-2.42	
	B3LYP/6-31+G(d,p)/LANL2DZdp	-2.60		-2.52		-2.82		-1.60	

10.1002/anie.202012262

All values are presented in kcal/mol. *Interaction energy (IE) is computed as the difference between the complex and the isolated constituents in the same geometry as the complex. ** Complexation energy (CE) is computed as the difference between the energy of the complex and that of the isolated constituents in their minima configuration. Both IE and CE were computed using chloride and were corrected for basis set superposition error using the counterpoise technique[46] (see SI for more details).

Interaction energy analysis

Interaction energies for the HBeXB model compounds (**1, 3, 5, 7**) and the non-hydrogen bonding controls (**2, 4, 6, 8**) with chloride were computed to further assess the impact of an intramolecular hydrogen bond on halogen bond strength (see SI for details).[46] Chloride was chosen as the anion for this analysis for computational simplicity. The interaction energies correlated with the σ-hole analysis (Table S1 and S2 in SI on page S36 & S37). For example, the strongest charge-assisted halogen bond occurred with the fluoro HBeXB derivative **5**, the species with the most positive σ-hole. Likewise, the weakest halogen bond of the pyridinium derivatives occurred with the non-hydrogen bonding methyl derivative **2** which also had the smallest $V_{s,max}$. The largest difference in interaction energies (a measure of HBeXB amplification) between pyridinium HBeXB donors and the non-hydrogen bonding derivatives occurred with the most electron-rich pair (**1** & **2**). Here,

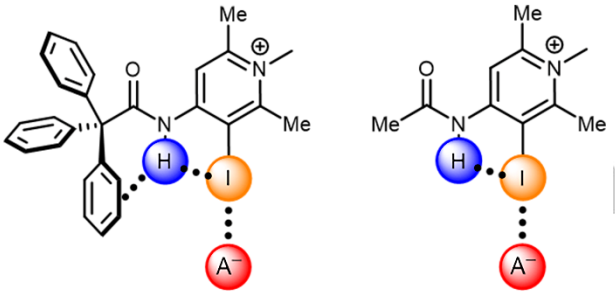

Figure 4. ChemDraw depictions of bifurcated hydrogen bonding in the trityl derivative (**1**) and monodentate hydrogen bonding in the methyl derivative (**1-methyl**).

there was a 1.01 kcal/mol HBeXB enhancement, whereas the proto (**3** & **4**) and fluoro (**5** & **6**) derivatives exhibited smaller differences in interaction energies by 0.47 and 0.17 kcal/mol, respectively. This trend further highlights that electron-rich halogen bond donors are influenced more by an adjacent hydrogen bond. Analysis of the neutral trifluoro derivatives provides more evidence, where the amide derivative **7** (HBeXB) has a stronger interaction energy with chloride than **8** (no intramolecular hydrogen bond) by 1.44 kcal/mol.

Next, we considered what factors may be limiting HBeXB enhancement in this model system. The local environment surrounding the hydrogen bond donor is congested and the amide protons of **1, 3, 5, & 7** can be described as bifurcated donors (Figure 4), having contacts with the π-electron system of a phenyl ring and the iodine halogen bond donor. As such, we considered the implications of hydrogen bond bifurcation on the HBeXB, to evaluate if approximately 1.4 kcal/mol is the upper limit to HBeXB amplification. To test this, interaction energies were calculated for derivatives of **1–4,** where the trityl group was replaced with a methyl group (Figure 4, for additional details see SI). Interestingly, the methyl derivatives, with monodentate hydrogen bonds, led to a greater enhancement of halogen bond strength. The Δ interaction energies were 2.70 kcal/mol for the **3-methyl** & **4-methyl** derivatives and 3.02 kcal/mol for the **1-methyl** & **2-methyl** derivatives (Table S2 in SI). The enhanced halogen bonding is attributed to the monodentate amide hydrogen bond donor of the methyl derivatives (Figure 4). This is the first evidence that stronger hydrogen bond donors will provide greater improvement of halogen bond strength in HBeXBs. The data presented here indicates that halogen bonds can be enhanced by up to 3 kcal/mol per iodine halogen bond donor in this system (gas-phase DFT analysis) when accepting a single amide hydrogen bond.[47] However, altering the angle of the hydrogen bond may also influence the halogen bond and will be considered in future studies.

Comparison to substituent effects

Substituent effects are a standard method used to enhance halogen bond strength. Appending electron withdrawing groups typically strengthens the halogen bond while electron donating groups have the opposite effect. To contextualize the HBeXB, interaction energies were calculated for two iodobenzene derivatives (see SI) and compared to the HBeXB augmentation described *vida infra* at the same level of theory. The halogen bonding interaction energy of 4-fluoroiodobenzene with chloride was 2.60 kcal/mol greater than iodobenzene with chloride. For comparison, the HBeXB enhancement for the **1-methyl** & **2-methyl** derivatives noted above was 3.02 kcal/mol. Thus, the enhancement from an HBeXB can be greater than introducing a fluorine atom to the *para* position of iodobenzene.

Other Functionals & Complexation Energy

While B3LYP has shown good agreement between calculated and experimental binding[48,49] we also carried out all the calculations using the M06-2X and ωb97xd functionals with the def2-TZVPP basis set for comparison. All the calculations highlight that the HBeXB augments the halogen bond. For the M06-2X and ωb97xd calculations the $\Delta V_{s,max}$ ranges from 1.76-5.52 kcal/mol and the ΔIEs range from -0.56-(-1.81) kcal/mol (Table 1 and Table S1 and S2). The trends in the data for the interaction energy calculations with the M06-2X and ωb97xd functionals parallel the B3LYP results described above showing that the more electron rich HBeXB compounds (**1**-**6**) enhance the halogen bond the most.

Complexation energies were also calculated as another method of evaluating the HBeXB that accounts for ligand deformation upon binding. Regardless of computational method, the HBeXB derivatives led to more stable complexes than the non-hydrogen bonding derivatives. Differences in complexation energies were -2.10-(-3.39) kcal/mol within the pyridinium family (**1**-**6**, Table 1) and -1.60-(-2.42) kcal/mol for the neutral species (**7**-**8**, Table 1). This further highlights that an adjacent hydrogen bond enhances the halogen bond.

For the $V_{s,max}$ and complexation energy calculations we note a slight difference in data trends when using the M06-2X and ωb97xd functionals as compared to the B3LYP calculations. This deviation is attributed to the notably different ester conformations (when not bound to chloride) when using M06-2X and ωb97xd (Figure S27). The M06-2X and ωb97xd functionals include

10.1002/anie.202012262

dispersion effects and thus the esters in these calculations display π-stacking between the pyridinium and one of the trityl aromatic rings. Nevertheless, the HBeXB strengthens the halogen bond in every case.

Structural evaluations of HBeXB and XB systems

Triflate salts of **1** & **2** were synthesized (see SI) and crystal structures with halides (chloride, bromide, and iodide) were obtained, affording the first assessment of isostructural monodentate HBeXB and non-hydrogen bonding pairs in the solid-state (Figure 5; for crystallization and crystallographic details see SI).[50]

Halide crystal structures of **1** reaffirm that the trityl group prevents intermolecular hydrogen bonding and facilitates intramolecular hydrogen bonding to the iodine donors (parameters shown in Table 2). Previous theoretical investigations have indicated that larger halogens have a wide range (~40-180°) of favorable hydrogen bond contact angles.[38] The H•••I—C angles 61.2(5)°, 61.8(6)°, and 60.8(6)° for the chloride, bromide, and iodide complexes of **1,** respectively, are within this range. Systematically, halogen bond contacts for HBeXB (**1**) with halides are shorter (or in the case of chloride similar) than halide structures of the non-hydrogen bonding **2**, despite being less linear (Table 2). Specifically, the bromide and iodide structures of **1•Br⁻** and **1•I⁻** are roughly 0.058 Å and 0.076 Å shorter than **2•Br⁻**, and **2•I⁻**, even though the contact angles are less linear by about 9.6° and 7°, respectively. The **1•Cl⁻** and **2•Cl⁻** halogen bond distances are within the standard uncertainty of the measurements and have a difference in halogen bond angle of ≈ 2°. The similar halogen bond distances in **1•Cl⁻** and **2•Cl⁻** is attributed to the fact that these halogen bond contacts are already quite close (reduction ratios for both are 0.77—for definition of reduction ratio see table 2 footer). This is in contrast with the bromide and iodide structures where the reduction ratios of the non-hydrogen bonding ester derivatives are 0.82 (**2•Br⁻**) and 0.83 (**2•I⁻**). The HBeXB reduces the reduction ratios to 0.80 (**1•Br⁻**) and 0.81 (**1•I⁻**). *Thus, these halide crystal structures highlight that hydrogen bonding to halogen bond donors strengthens halogen bonds in the solid-state.*

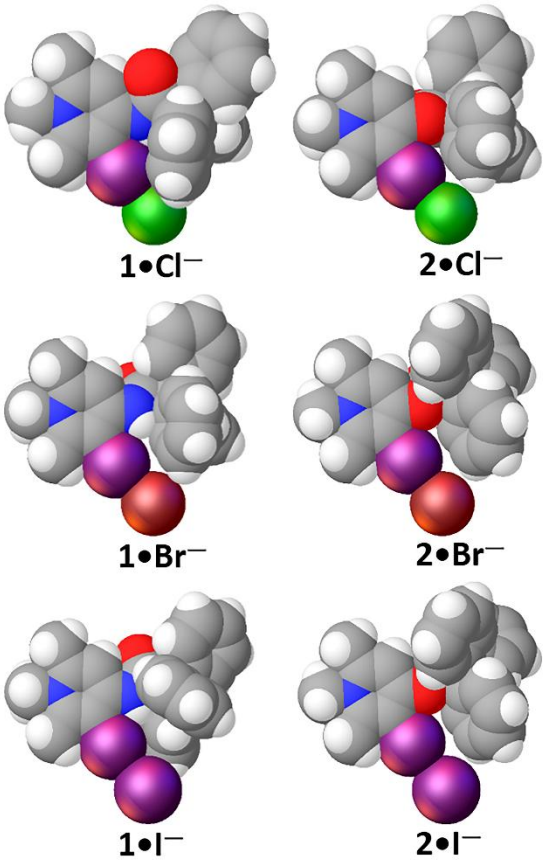

Figure 5. Asymmetric units of HBeXB and non-hydrogen bonding pairs highlighting an isostructural nature. Sphere packing diagrams drawn using default van der Waals radii in Olex2. Anion colors: chloride = green, bromide = maroon, iodide = purple.

Differing C–H hydrogen bond patterns between the chloride and iodide structures of **1** and **2** led to subtle conformational differences that affected the environment around the anions. For example, the C–H group *meta* to the pyridinium nitrogen contacts the halide in all three structures of **2** (Figure S25). In contrast, in **1•Cl⁻** and **1•I⁻** the pyridinium C–H donor forms an intramolecular hydrogen bond with the carbonyl oxygen. Nevertheless, both the **1•Br⁻** and **2•Br⁻** structures have similar conformations that provides compelling evidence that the contraction of the halogen bond in the **1•anion** complexes is due to the amide hydrogen bond to the iodine. The **1•Br⁻** and **2•Br⁻** structures both have C—H•••Br⁻ contacts (2.7426(3)Å and 158.48(11)° for **1•Br⁻**, and 2.7846(4)Å and 155.44(12)° for **2•Br⁻**) yet, the halogen bond distance in **1•Br⁻** is shorter than in **2•Br⁻**. Thus, small differences in packing and receptor conformation do not explain the shorter halogen bonds in the HBeXB derivatives (**1•I⁻** &**1•Br⁻**), rather the HBeXB strengthens binding and produces shorter contacts in the solid-state. [51]

Table 2. Summary of Germane Geometrical Parameters

Complex	XB Interaction	XB Distance (Å)	XB Angle (°)	R_{XA}[#]	N—H•••I distance (Å)	N—H•••I angle (°)
1•Cl⁻	I•••Cl⁻	2.9808(7)	170.66(6)	0.77	2.64(2)	125(3)
2•Cl⁻	I•••Cl⁻	2.982(2)	172.9(2)	0.77	—	—
1•Br⁻	I•••Br⁻	3.1265(4)	169.06(5)	0.80	2.86(3)	107(2)
2•Br⁻	I•••Br⁻	3.1850(5)	178.68(4)	0.82	—	—
1•I⁻	I•••I⁻	3.3113(5)	171.43(9)	0.81	2.66(3)	125(3)
2•I⁻	I•••I⁻	3.3879(3)	178.40(7)	0.83	—	—

[#]R_{XA} is the reduction ratio which is defined as $R_{XA} = \frac{d_{XA}}{(X_{vdW} + A_{vdW})}$ where d_{XA} is the measured distance (Å) from the halogen donor (X) to the acceptor (A), divided by the sum of the van der Waals radii (Å) of X and A (X_{vdW}+ A_{vdW}). Van der Waals radii used from Alvarez.[51]

Solution evaluation of the HBeXB

The theoretical analysis herein indicated that the most electron-rich HBeXB and non-hydrogen bonded pairs (**1**, **2** and **7**, **8**) should provide the greatest differences in binding and allow for an isolated monodentate HBeXB to be measured in solution for the first time. To test this, titration experiments with chloride were carried out under the hypothesis that HBeXB compounds would result in greater association constants. Regrettably, **1** and **2** were hampered by solubility issues and decomposition, preventing solution assessment. Fortunately, **7** and **8** were not affected by the same challenges. Association constants for **7** and **8** with chloride (tetra-*n*-butylammonium chloride, TBACl) were measured by ^{19}F NMR titrations at 25° C. Acetone-d_6 was used as the solvent based on reports by Taylor who showed that this medium produced the greatest binding between TBACl and neutral halogen bond donors.[52,53] Likewise, these studies also indicated that chloride produces the greatest halide binding constants with neutral halogen bond donors. Halogen bonding of **7** and **8** to chloride was confirmed by the upfield shift of the fluorine signals upon addition of TBACl.[54] Association constants were determined using BINDFIT,[54] and the data was modeled to a 1:1 binding stoichiometry (see SI for further details). The non-hydrogen bonding derivative (**8**) halogen bonds to chloride with an association constant of 35.7 M^{-1}, which is consistent with other charge-neutral halogen bonding molecules in solution. In contrast, the isostructural HBeXB derivative, **7**, showed a marked increase in halogen bonding strength with an association constant of 43.3 M^{-1}. After replicating the experiment four times a rough estimate of the spread was obtained by multiplying the standard deviation by two to obtain an approximation of the 95% confidence interval.[55] Treatment of the data in this manner led to interval values of [47.0, 39.8] and [37.9, 33.4] for **7** and **8**, respectively (Table 3). Thus, the derivative with the HBeXB (**7**) exhibits stronger binding in solution when compared to the non-hydrogen bonding control which is fully consistent with the theoretical and solid-state findings.

To rule out possible direct intermolecular amide hydrogen bonding of **7** to chloride, ^{1}H NMR data were collected in the presence of increasing equivalents (≈ 21.3 equivalents) of TBACl in acetone-d_6. A common indication of hydrogen bonding is the downfield shift of the proton resonance upon complexation. The amide proton signal of **7** shifted only 0.16 ppm downfield. For comparison, a derivative of **7** was synthesized that *would* allow for intermolecular hydrogen bonding to chloride (**9**, a hydrogen in place of the iodine, Figure 3, and Figure S26). Compound **9** exhibited a much larger 0.72 ppm shift downfield in the presence of slightly fewer equivalents of TBACl (≈ 20.7 equivalents of TBACl). Fitting this ^{1}H NMR data to a binding constant highlights that **9** binds chloride quite weakly with an association constant of 12.8 M^{-1}. This weak binding coupled with the fact that the shift of the amide hydrogen in **9** is 4.5 times greater than **7** suggests that the amide hydrogen in **7** does not directly hydrogen bond to chloride in solution (See SI).

Table 3. Solution association constants

Compound	K_a*	95% confidence interval**
7	43.3	[47.0, 39.8]
8	35.7	[37.9, 33.4]
9	12.8***	n.d.

*K_a values between TBACl and 7 and 8 measured by ^{19}F NMR titrations at 25° C in acetone-d_6. The mean was derived from 4 experiments. **approximation of the 95% confidence interval obtained by multiplying the standard deviation by two. *** K_a value obtained from a single ^{1}H titration at 25° C in acetone-d_6.

This conclusion is further supported by the severe steric congestion of the amide in **7**, as demonstrated in the theoretical and solid-state analyses. Collectively, the evidence indicates that the amide proton is not a considerable 'direct' contributor (i.e. hydrogen bonding to chloride) to the association constant, and likely does not account for the increased affinity observed between **7** and **8**. Thus, the solution data reveal that the hydrogen bond augments halogen bonding in solution.

Conclusion

The first experimental quantification of a monodentate HBeXB has revealed several new fundamental features. Solid-state structures highlight that HBeXB analogues form shorter halogen bonds with bromide and iodide, despite a less linear interaction when compared to non-hydrogen bonding controls. ^{19}F NMR titrations of neutral fluorinated derivatives showed that HBeXB derivative (**7**) bound chloride stronger than a similar derivative that does not have a hydrogen bond (**8**), at a (approximate) 95% confidence interval. Theoretical studies indicated that HBeXB amplification is likely greater in more electron-rich systems where

the halogen (iodine) is less polarized. Comparison of the trityl species (with a bifurcated amide hydrogen bond) to methyl derivatives (with a monodentate amide hydrogen bond) suggested that the strength of a halogen bond can be fine-tuned by varying the strength of an adjacent hydrogen bond. Interaction energies with chloride showed that with monodentate iodine halogen bond donors can be strengthened by up to 3 kcal/mol when concurrently accepting a single intramolecular amide hydrogen bond—an enhancement comparable to introducing a *para*-fluorine substituent to iodobenzene. Collectively, the data presented here form the foundation for future studies of organohalogen hydrogen bond acceptors and HBeXBs.

The studies herein demonstrate the significance of a halogen operating simultaneously as a halogen bond donor (C—X•••LB) and a hydrogen bond (H•••X—C) acceptor, leading to several outlooks. Consider again the debated importance of hydrogen bonding (H•••X—C) and halogen bonding (C—X•••LB) in protein-ligand interactions. While the degree of significance likely depends on the circumstances, the HBeXB should be considered in future analyses as its effects will be amplified and occur more frequently in environments where solvent effects are limited, and conformational flexibility is muted (i.e. protein-ligand complexes). The implications of the HBeXB are further heightened when one considers that over half of all launched organohalogen drugs contain heavy halogens (X= Cl, Br, I) with the capacity for halogen bonding.[56] In synthetic supramolecular systems, HBeXB effects will be pronounced when multidentate hydrogen and halogen bond donors are employed—as demonstrated by the preorganization of anion receptors.[41] Our results also show that amplification from the HBeXB is comparable to substituent effects and that the enhancement in halogen bond strength is likely more evident in electron rich systems. This suggests that HBeXBs may permit one to utilize a more stable halogen bond donor while maintaining a stronger halogen bonding interaction.[57] Overall, continued studies of HBeXBs will enrich our grasp of the chemical relationship between hydrogens and halogens and refine our understanding of halogen bond properties and the puzzling behavior of late group 17 hydrogen bond acceptors.

Acknowledgements

OBB, DAD, AMSR, & JHM are thankful for the support from National Science Foundation (NSF) CAREER CHE-1555324. OBB, DAD, AMSR, & JHM are thankful for the X-ray Core facility support by the Center for Biomolecular Structure and Dynamics CoBRE (NIH NIGMS grant P20GM103546), and the University of Montana (UM). The X-ray crystallographic data were collected using a Bruker D8 Venture, principally supported by NSF MRI CHE-1337908. V.S.B. was supported by the US Department of Energy, Office of Science, Basic Energy Sciences, Chemical Sciences, Geosciences, and Biosciences Division. This research used resources of the Compute and Data Environment for Science (CADES) at the Oak Ridge National Laboratory, which is supported by the Office of Science of the U.S. Department of Energy under Contract No. DE-AC05-00OR22725.

Keywords: Hydrogen Bonds • Halogen Bonds • Noncovalent Cooperativity • Supramolecular Chemistry • Bond Theory

[1] G. Desiraju, T. Steiner, *The Weak Hydrogen Bond*, Oxford University Press, **2001**.

[2] The modest hydrogen bond acceptor performance of fluorine atoms has been attributed to several physical characteristics. Yet the rationales for fluorine do not appropriately describe the traits of heavier halogens. For a more detailed discussion see SI.

[3] H.-J. Schneider, *Chem. Sci.* **2012**, *3*, 1381.

[4] R. Taylor, *Acta Crystallogr. Sect. B Struct. Sci. Cryst. Eng. Mater.* **2017**, *73*, 474–488.

[5] C. Dalvit, C. Invernizzi, A. Vulpetti, *Chem. Eur. J.* **2014**, *20*, 11058–11068.

[6] J. D. Dunitz, R. Taylor, *Chem. Eur. J.* **1997**, *3*, 89–98.

[7] J. A. K. Howard, V. J. Hoy, D. O'Hagan, G. T. Smith, *Tetrahedron* **1996**, *52*, 12613–12622.

[8] J. D. Dunitz, *ChemBioChem* **2004**, *5*, 614–621.

[9] J. Nadas, S. Vukovic, B. P. Hay, *Comput. Theor. Chem.* **2012**, *988*, 75–80.

[10] P. Matczak, *Mol. Phys.* **2017**, *115*, 364–378.

[11] A. Kovács, Z. Varga, *Coord. Chem. Rev.* **2006**, *250*, 710–727.

[12] Y. H. Liu, X. N. Xu, X. Zhao, Z. T. Li, *Supramol. Chem.* **2015**, *27*, 310–320.

[13] P. A. Robertson, L. Villani, U. L. M. Dissanayake, L. F. Duncan, B. M. Abbott, D. J. D. Wilson, E. G. Robertson, *Phys. Chem. Chem. Phys.* **2018**, *20*, 8218–8227.

[14] J. Shang, N. M. Gallagher, F. Bie, Q. Li, Y. Che, Y. Wang, H. Jiang, *J. Org. Chem.* **2014**, *79*, 5134–5144.

[15] B. Y. Lu, Z. M. Li, Y. Y. Zhu, X. Zhao, Z. T. Li, *Tetrahedron* **2012**, *68*, 8857–8862.

[16] C. Lu, B. Htan, S. Fu, C. Ma, Q. Gan, *Tetrahedron* **2019**, *75*, 4010–4016.

[17] Z. R. Laughrey, T. G. Upton, B. C. Gibb, *Chem. Commun.* **2006**, 970.

[18] C. L. D. Gibb, E. D. Stevens, B. C. Gibb, *J. Am. Chem. Soc.* **2001**, *123*, 5849–5850.

[19] L. Brammer, E. A. Bruton, P. Sherwood, *Cryst. Growth Des.* **2001**, *1*, 277–290.

[20] J.-A. van den Berg, K. R. Seddon, *Cryst. Growth Des.* **2003**, *3*, 643–661.

[21] G. R. Desiraju, P. S. Ho, L. Kloo, A. C. Legon, R. Marquardt, P. Metrangolo, P. Politzer, G. Resnati, K. Rissanen, *Pure Appl. Chem.* **2013**, *85*, 1711–1713.

[22] G. Cavallo, P. Metrangolo, R. Milani, T. Pilati, A. Priimagi, G. Resnati, G. Terraneo, *Chem. Rev.* **2016**, *116*, 2478–2601.

[23] G. Cavallo, P. Metrangolo, T. Pilati, G. Resnati, M. Sansotera, G. Terraneo, *Chem. Soc. Rev.* **2010**, *39*, 3772–3783.

[24] M. Fourmigué, *Curr. Opin. Solid State Mater. Sci.* **2009**, *13*, 36–45.

[25] J. C. Christopherson, F. Topić, C. J. Barrett, T. Friščić, *Cryst. Growth Des.* **2018**, *18*, 1245–1259.

[26] L. C. Gilday, S. W. Robinson, T. A. Barendt, M. J. Langton, B. R. Mullaney, P. D. Beer, *Chem. Rev.* **2015**, *115*, 7118–7195.

[27] B. Li, S. Q. Zang, L. Y. Wang, T. C. W. Mak, *Coord. Chem. Rev.* **2016**, *308*, 1–21.

[28] A. Mukherjee, S. Tothadi, G. R. Desiraju, *Acc. Chem. Res.* **2014**,

47, 2514–2524.

[29] P. Metrangolo, T. Pilati, G. Terraneo, S. Biella, G. Resnati, *CrystEngComm* **2009**, *11*, 1187.

[30] X. Ding, M. Tuikka, M. Haukk, in *Recent Adv. Crystallogr.*, InTech, **2012**, p. 13.

[31] P. Auffinger, F. A. Hays, E. Westhof, P. S. Ho, *Proc. Natl. Acad. Sci.* **2004**, *101*, 16789–16794.

[32] N. Ramasubbu, R. Parthasarathy, P. Murray-Rust, *J. Am. Chem. Soc.* **1986**, *108*, 4308–4314.

[33] P. Von R. Schleyer, R. West, *J. Am. Chem. Soc.* **1959**, *81*, 3164–3165.

[34] J. M. Ontoria, E. H. Rydberg, S. Di Marco, L. Tomei, B. Attenni, S. Malancona, J. I. Martin Hernando, N. Gennari, U. Koch, F. Narjes, M. Rowley, V. Summa, S. S. Carroll, D. B. Olsen, R. De Francesco, S. Altamura, G. Migliaccio, A. Carfì, *J. Med. Chem.* **2009**, *52*, 5217–5227.

[35] E. I. Howard, R. Sanishvili, R. E. Cachau, A. Mitschler, B. Chevrier, P. Barth, V. Lamour, M. Van Zandt, E. Sibley, C. Bon, D. Moras, T. R. Schneider, A. Joachimiak, A. Podjarny, *Proteins Struct. Funct. Genet.* **2004**, *55*, 792–804.

[36] Y. Lu, Y. Wang, Z. Xu, X. Yan, X. Luo, H. Jiang, W. Zhu, *J. Phys. Chem. B* **2009**, *113*, 12615–12621.

[37] Y. Lu, Y. Wang, W. Zhu, *Phys. Chem. Chem. Phys.* **2010**, *12*, 4543–4551.

[38] F. Y. Lin, A. D. Mackerell, *J. Phys. Chem. B* **2017**, *121*, 6813–6821.

[39] A. M. S. Riel, R. K. Rowe, E. N. Ho, A.-C. C. Carlsson, A. K. Rappé, O. B. Berryman, P. S. Ho, *Acc. Chem. Res.* **2019**, *52*, 2870–2880.

[40] A.-C. C. Carlsson, M. R. Scholfield, R. K. Rowe, M. C. Ford, A. T. Alexander, R. A. Mehl, P. S. Ho, *Biochemistry* **2018**, *57*, 4135–4147.

[41] A. M. S. Riel, D. A. Decato, J. Sun, C. J. Massena, M. J. Jessop, O. B. Berryman, *Chem. Sci.* **2018**, *9*, 5828–5836.

[42] Y. Y. Zhu, L. Jiang, Z. T. Li, *CrystEngComm* **2009**, *11*, 235–238.

[43] Y.-Y. Y. Zhu, H.-P. P. Yi, C. Li, X.-K. K. Jiang, Z.-T. T. Li, *Cryst. Growth Des.* **2008**, *8*, 1294–1300.

[44] D. Y. Wang, J. L. Wang, D. W. Zhang, Z. T. Li, *Sci. China Chem.* **2012**, *55*, 2018–2026.

[45] M. J. Frisch, G. W. Trucks, H. B. Schlegel, G. E. Scuseria, M. A. Robb, J. R. Cheeseman, G. Scalmani, V. Barone, B. Mennucci, G. A. Petersson, H. Nakatsuji, M. Caricato, X. Li, H. P. Hratchian, A. F. Izmaylov, J. Bloino, G. Zheng, J. L. Sonnenberg, M. Hada, M. Ehara, K. Toyota, R. Fukuda, J. Hasegawa, M. Ishida, T. Nakajima, Y. Honda, O. Kitao, H. Nakai, T. Vreven, J. A. J. Montgomery, J. E. Peralta, F. Ogliaro, M. Bearpark, J. J. Heyd, E. Brothers, K. N. Kudin, V. N. Staroverov, R. Kobayashi, J. Normand, K. Raghavachari, A. Rendell, J. C. Burant, S. S. Iyengar, J. Tomasi, M. Cossi, N. Rega, N. J. Millam, M. Klene, J. E. Knox, J. B. Cross, V. Bakken, C. Adamo, J. Jaramillo, R. Gomperts, R. E. Stratmann, O. Yazyev, A. J. Austin, R. Cammi, C. Pomelli, J. W. Ochterski, R. L. Martin, K. Morokuma, V. G. Zakrzewski, G. A. Voth, P. Salvador, J. J. Dannenberg, S. Dapprich, A. D. Daniels, O. Farkas, J. B. Foresman, J. V. Ortiz, J. Cioslowski, D. J. Fox, **2009**.

[46] S. F. Boys, F. Bernardi, *Mol. Phys.* **1970**, *19*, 553–566.

[47] The lone pair of electrons on the ester oxygen may contribute to a weakening of the halogen bond though electron pair repulsion. thus, the value we suggest here may be an upper limit estimate.

[48] M. G. Sarwar, B. Dragisic, L. J. Salsberg, C. Gouliaras, M. S. Taylor, *J. Am. Chem. Soc.* **2010**, *132*, 1646–1653.

[49] M. G. Chudzinski, M. S. Taylor, *J. Org. Chem.* **2012**, *77*, 3483–3491.

[50] Deposition numbers 2003671-2003676 & 2023532 contain the supplementary crystallographic data for this paper. These data are provided free of charge by the joint cambridge crystallographic data centre and fachinformationszentrum karlsruhe access structures service www.ccdc.cam.ac.uk/

[51] S. Alvarez, *Dalt. Trans.* **2013**, *42*, 8617.

[52] M. S. Taylor, *Coord. Chem. Rev.* **2020**, *413*, 213270.

[53] M. G. Sarwar, B. Dragisić, E. Dimitrijević, M. S. Taylor, *Chem. Eur. J.* **2013**, *19*, 2050–2058.

[54] D. von der Heiden, A. Vanderkooy, M. Erdélyi, *Coord. Chem. Rev.* **2020**, *407*, 213147.

[55] P. Thordarson, *Chem. Soc. Rev.* **2011**, *40*, 1305–1323.

[56] Z. Xu, Z. Yang, Y. Liu, Y. Lu, K. Chen, W. Zhu, *J. Chem. Inf. Model.* **2014**, *54*, 69–78.

[57] R. L. Sutar, S. M. Huber, *ACS Catal.* **2019**, *9*, 9622–9639.

10.1002/anie.202012262

Entry for the Table of Contents

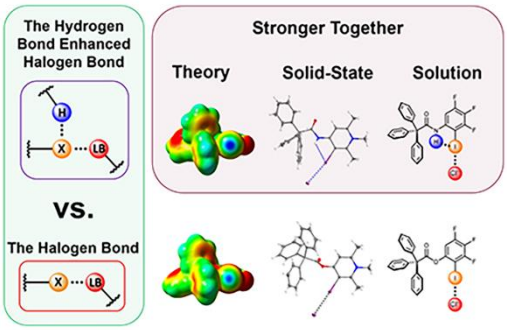

Stronger Together: The amount that a hydrogen bond to an iodine donor strengthens the resulting halogen bond is quantified for the first time.